19th Brazilian Congress of Thermal Sciences and Engineering
November 06th-10th, 2022, Bento Gonçalves - RS - Brazil

ENC-2022-0370
CFD ASSESSMENT OF THE THERMO-HYDRAULIC PERFORMANCE CHARACTERISTICS OF TUBE-FIN HEAT EXCHANGERS

Márcio J. E. Demétrio
João V. L. Hinterholz
Luiz P. B. Braun
Christian J. L. Hermes
POLO Labs, Departamento de Engenharia Mecânica, Universidade Federal de Santa Catarina, Florianópolis-SC, Brasil
marcio.demetrio@polo.ufsc.br

Abstract. *The present work is aimed at developing a computational method, using CFD techniques, to characterize the thermo-hydraulic performance of fin tube heat exchangers for light commercial refrigeration applications. The objective behind this work is to reduce the number of prototypes and wind tunnel tests, but at the same time be able to obtain through computational simulations the characteristics curves of pressure drop and heat transfer coefficient as a functions of volumetric flow rate, and also the Fanning friction factor (f) and Colburn factor (j) as a function of Reynolds number. The CFD models lead to results with a 20% difference in terms of pressure drop for the experimental test, and an error lower than 5% in the total heat exchange. Also, simplified versions of the model were able to reproduce the results of the full models mainly in those cases where the airflow section is uniform.*

Keywords: *Condenser, Evaporator, J-factor, Friction factor, CFD, Tube-fin.*

1. INTRODUCTION

Given the importance of heat exchangers in the refrigeration cycle performance, improvements in this component's efficiency can substantially influence the global performance of the system, reducing external irreversibility and reflecting into a lower energy consumption. Therefore, studies regarding fin tube heat exchangers are relevant due to their broad application in refrigerators that comprise a large market share, since domestic applications until commercial and air conditioning ones. These exchangers are characterized by having large heat transfer surfaces per unit volume. They are generally used when at least one of the fluids is a gas and is therefore characterized by low convective heat transfer coefficients. In these types of exchangers, the large heat exchange area tries to compensate for the low heat transfer coefficient on the gas side. Nowadays, some of the main characteristics of heat exchangers, like the pressure drop curves (ΔP) and heat transfer coefficients (UA) as a function of volumetric flow ($\dot{V}$), are obtained through standardized test in wind tunnels, which are onerous and time consuming. Besides that, such tests demand prototypes, which further increases the cost of product development.

Aiming to reduce the need of experimental tests, the present work has the objective to develop a computational method using CFD (Computational Fluid Dynamics) to characterize the thermos-hydraulic performance of tube-fin heat exchangers for light commercial refrigeration applications. In this regard, the characteristic curves are numerically regressed to obtain the functions that relate the Fanning (f) and Colburn (j) factors with the Reynolds number in the flow through the center of the heat exchanger (Re). Such approach was employed by Barbosa et al. (2010), who made a computational study focusing on "no-frost" evaporators typically employed in domestic refrigerators. Besides making possible to obtain the characteristic curves of the no-frost heat exchangers, the simulation results showed that around 40% of all the heat exchange is made in the first segment, that corresponds to about 20% of the heat exchanger's area.

Such results, however, are restricted to the studied evaporators, that substantially differ both in geometry and in operation conditions from the tube-fin heat exchangers employed in commercial refrigerators. While the evaporators are known to operate in low volumetric flow, low compactness, and high aspect ratio, i.e., long longitudinal length and reduced face area, the tube-fin heat exchangers conventionally employed in commercial refrigeration systems operate with high volumetric flow, high compactness and low aspect ratio, i.e., large face area and reduced length.

In this context, the present work intends to develop and validate a computational approach, through CFD techniques, that can be employed to obtain thermos-hydraulic performance curves for fin tube heat exchangers operating in commercial refrigeration conditions.

2. EXPERIMENTAL WORK

Any computer simulation work requires experimental data for calibration and to validate the models. For the fluid dynamic analysis of the heat exchangers used in this work, i.e., to obtain the ΔP curves as a function of the volumetric flow ($\dot{V}$), an open wind tunnel was employed, built on according to the specifications of the ASHRAE (1987, 2000) standards, accordingly Figure 1 (left). The tunnel is composed of several internal sections, pressure and temperature's measurement points, it is equipped with a variable rotation booster (A), a dampers system (B), that acts in the fan's volumetric flow control, a nozzle plate (C), differential pressure transducers (D) for the volumetric flow calculations and drilled nets (E) to homogenize the air flow before the test section (F).

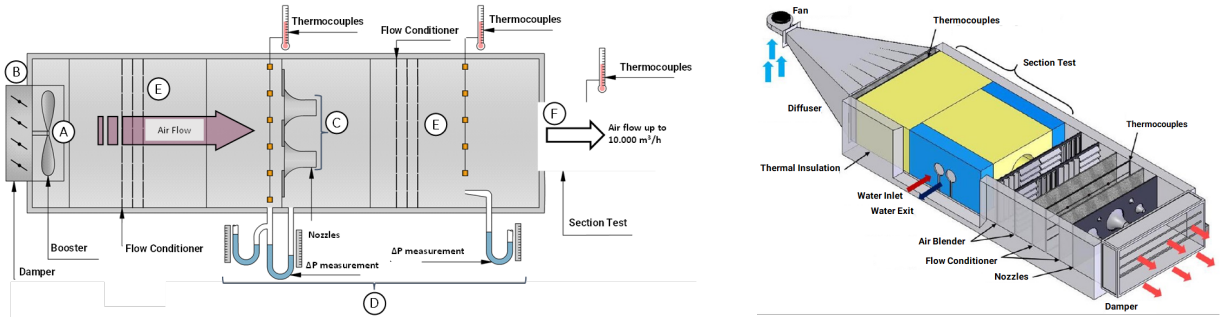

Figure 1. Aerodynamic wind tunnel (left) and thermal wind tunnel (right).

Regarding the thermal analysis of the heat exchangers employed in this work, i.e., the obtention of UA curves as a function of volumetric flow, the thermal wind tunnel employed was projected on according to the ASHRAE (1987, 1988, 1999) standards and is shown in Figure 1 (right). The tunnel is composed of two circuits: the air circuit and a closed water circuit (which flows through the tubes). The air circuit is composed of a centrifugal fan, an air diffuser, the test section, and a nozzle plate to measure the volumetric flow. In order to assure that the flow is uniform in the test section, where the heat exchanger is installed, a felt net is placed right after the air diffuser. The test section is composed of a converging duct before the heat exchanger and another one, divergent, after it, to assure uniformity in the flow and to avoid by-pass, vortices formation and stagnation of the air flow passing though the heat exchanger. The water circuit has six components: two water pumps, the heat exchanger, a water filter, a mass flow transducer, and a thermostatic bath, to maintain a constant water temperature at the inlet of the heat exchanger. Through wind tunnel testing, the effectiveness of the heat exchanger can be determined by the following expression:

$$\epsilon = \frac{\frac{1}{2}(Q_w + Q_a)}{C_{min}\left(T_{w,in} - T_{a,in}\right)} \tag{1}$$

where C_{min} refers to the minimum thermal capacity rate between the two currents, i.e., air and water. The number of exchange units of the heat exchanger (N_{tu}) is calculated as a function of the effectiveness and of the ration between the minimum and maximum capacity rates through classic correlations for cross flow, with the air side not mixed and the water side mixed. The convection heat exchange coefficient on the air side can be obtained by:

$$\frac{1}{h} = \frac{A_s}{N_{tu}C_{min}} - \frac{A_s}{h_w A_{int}} \tag{2}$$

where A_s is the heat transfer area on the air side, including fins and tubes, h_w is the heat transfer coefficient on the water side, obtained through the Dittus-Boelter correlation, and A_{int} is the heat transfer area inside the tubes. After obtaining the characteristic curves, the heat transfer surface's parameters, j and f, can be determined from the following expressions:

$$f = \frac{A_{min}}{A_s}\frac{\rho}{\rho_{in}}\left[2\frac{\rho_{in}}{G^2}\Delta P - (1+\sigma^2)\left(\frac{\rho_{in}}{\rho_{out}} - 1\right)\right] \tag{3}$$

$$j = \frac{h}{Gc_p}Pr^{2/3} \tag{4}$$

where $\sigma = A_{min}/A_{face}$ is the fraction of free crossing area and $G = \dot{m}/A_{min}$ is the mass flow in the minimum crossing section, employed in the Reynolds number's evaluation in the core of the heat exchanger,

$$Re = \frac{GD_h}{\mu} \tag{5}$$

where $D_h = 4A_{min}L/A_s$ is the hydraulic diameter of the heat exchanger and μ the absolute viscosity of the air, evaluated through the average temperature between the inlet and the outlet, $\frac{1}{2}(T_{in} + T_{out})$, as well as the density ρ and the specific heat c_p. Several experimental tests with different heat exchanger configurations were executed, as described in the following sections.

2.1 Analyzed heat exchangers

In total, three heat exchangers, each with unique geometric characteristics, were studied. The main parameters of the heat exchangers are shown in Table 1. In all of them, the fins have an extension called "collar", whose function is to increase the heat transfer area with the heat pipes.

Table 1 – Geometric parameters of the heat exchangers

Parameter	Unit	HE01	HE02	HE03
		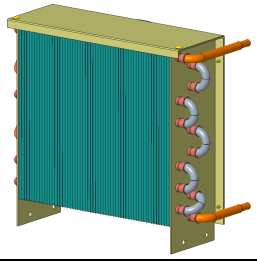	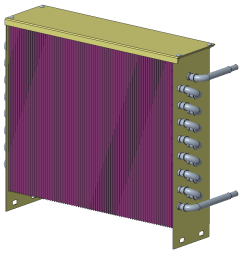	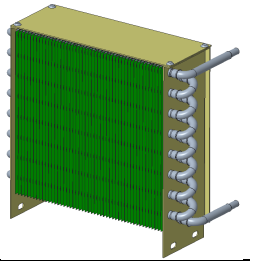
Nº Fins	-	62	71	59
Fins thickness	mm	0,125	0,15	0,125
Exchanger length	mm	216	305	216
A_{min}	mm^2	29592	44741	25375
A_s	mm^2	1065096	1550957	1012438
A_{face}	mm^2	43834	79331	43834
L	mm	44	44	44
σ	-	0,675	0,564	0,579
D_h	mm	4,89	5,08	4,41
V	mm^3	1928696	3490542	1928696

The heat exchanger 01 was experimentally tested only in the aerodynamic wind tunnel, while the heat exchangers 02 and 03 were also tested in the thermal wind tunnel.

3. METHOD AND RESULTS

3.1 Experimental/Numerical model HE01

Starting from the physical version of the heat exchanger, it was possible to build a complete CAD model of this heat exchanger. Some variations were studied, HE01.A, B, C and D, to evaluate the influence of the cross section of the tunnel in the results. The HE01.A corresponds to the original cross section of the tunnel, as in Figure 2 (left). In variants B and C, the cross section was reduced to 0,8 and 0,4m, respectively, while the D version had a constant section, as shown in Figure 2 (right).

In Figure 2, in addition to the dimensions of each model, the regions of each domain are also explained. The boundary condition in the inlet region was of prescribed velocity. The velocities used in the simulations were calculated from the volumetric flow data from the experiments. For the outlet region, a static pressure condition equal to zero was used. On

the sides of the tunnel, wall conditions were used, however, to compensate the impedance of the walls, a slip condition was used, that is, the friction of the walls was neglected. In this way, it is possible to reproduce the effect that the auxiliary fan promotes in the experiment.

The pressure drop behavior was analyzed as a function of volumetric flow for *Realizable K-Epsilon* turbulence model and its variations for wall treatment: *High y+* and *Two Layer*. In the regions near the inlet of the heat exchanger, on the fins and tubes and in the heat exchanger's outlet, mesh controls were employed. The density and dynamic viscosity properties used for the air were $\rho = 1{,}204\ \mathrm{kg/m^3}$ and $\mu = 1{,}825.10^{-5}$ Pa. s.

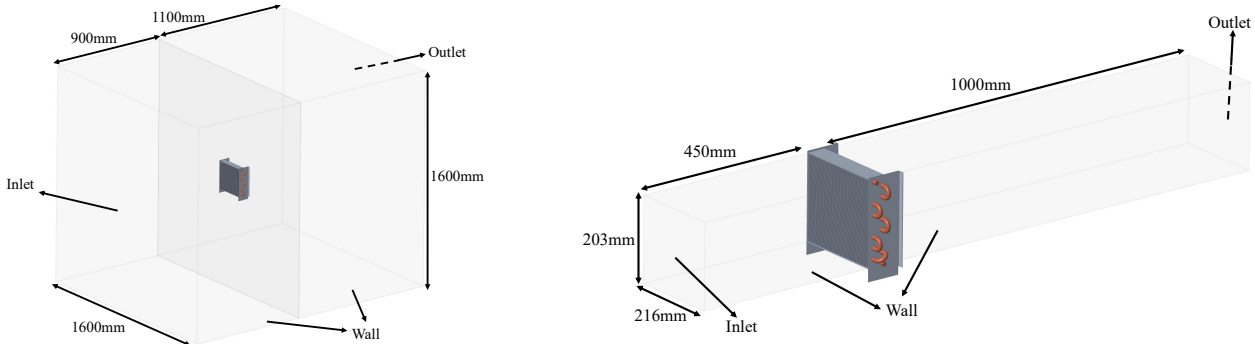

Figure 2. HE01.A on the left and HE01.D on the right.

The CFD simulations were made using the commercial software Simcenter STAR-CCM+, licensed for this laboratory. The choice for the *K-Epsilon* turbulence model is because it provides a good compromise between robustness, computational cost and precision, in addition to being a widely used model in industrial applications.

The *Realizable* variation was selected among other possibilities, such as the *Standard* one, due to its robustness in capturing flows with complex structures, rotation, boundary layer with adverse pressure gradient, separation, and recirculation. It's known that the boundary layer is formed in the regions close to the walls due to the flow. The highest gradients are found in these regions and the highest transfer rates occur there as well. Therefore, discretization this region is of paramount importance. Numerically, this region's treatment is done through wall functions and, depending on the y^+ ($y^+ = y\rho u/\mu$) value, the most appropriate wall function is chosen. In the previous equation, y represents the distance between the wall and the centroid of the first mesh element. To evaluate this region, two wall functions were studied in this work: *High y+* and *Two Layer*. The *High y+* wall function is used for $y^+ > 30$, while the *Two Layer* model is used for $1 > y^+ > 30$. Therefore, the *Two Layer* model can be used in situations where the mesh is composed of both refined and coarse regions.

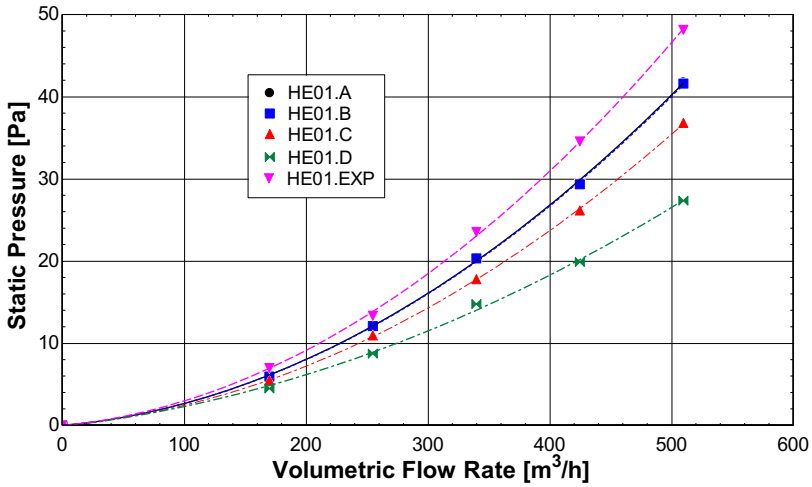

Figure 3. Comparative analysis between the experimental model and simulation versions of HE01 heat exchanger.

The results of the simulations for the HE01 model are disposed in Figure 3. It was found that the cross-section reduction for the B model had no impact on the pressure drop. However, for model C, there is a slight difference in relation to models A and B, that is, this suggests that from a minimum size, the flow cross section of the domain that leads air to the exchanger begins to influence the results. It is possible to observe that there is difference between the two simulations of the complete model HE01.A, because the version with the *Realizable K-Epsilon High y+* turbulence/wall model presented better results than the *Realizable K-Epsilon Two Layer* version. Finally, when models HE01.A and HE01.D are compared (considering both with the *Realizable K-Epsilon Two Layer* turbulence/wall model), the model HE01.A leads to a greater pressure drop, what was expected due to the contraction and expansion effects of the flow.

3.2 Experimental/Numerical model HE02

For the HE02, in the CFD simulations it was used the *Realizable K-Epsilon* turbulence model with the *High y+* wall treatment. Initially, the full version HE02.A was modelled according to the wind tunnel's dimensions (similar to the HE01.A model). From the gathered data it is possible to compare the results through the graphic shown in Figure 4. The simulation model is capable of reproducing fairly well the experimental results, with an error ranging from 5 to 15%.

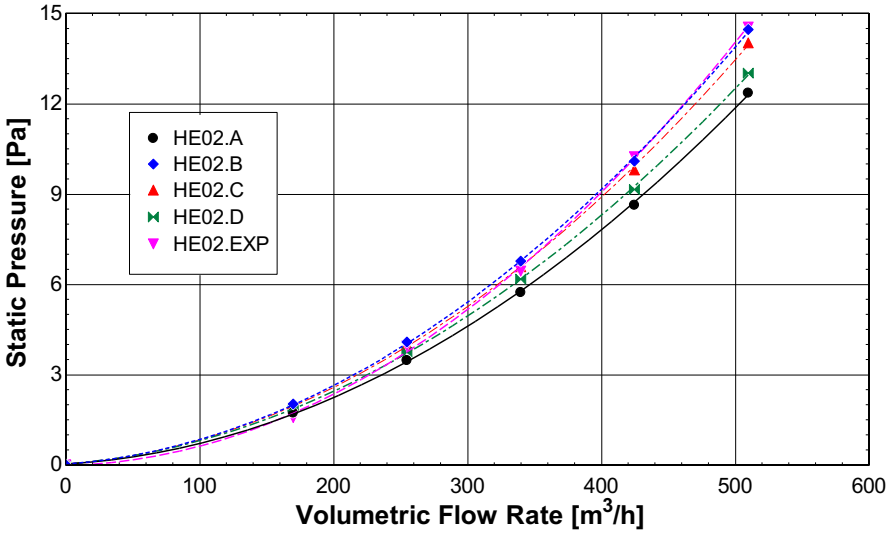

Figure 4. Comparison between the HE02.A model and the experimental analysis in an aerodynamic wind tunnel.

Simplified versions were also analyzed, aiming to reproduce the contraction and expansion effect due to the tunnel's shape, as shown in Figure 5 (left). In order to do so, rectangular inlet sections with different sections (models HE02.B, HE02.C and HE02.D) were tested. Besides that, still within the fluid dynamic study, constant section HE02.E (full model) and HE02.F (simplified version) configurations were also tested, as depicted in Figure 5 (right).

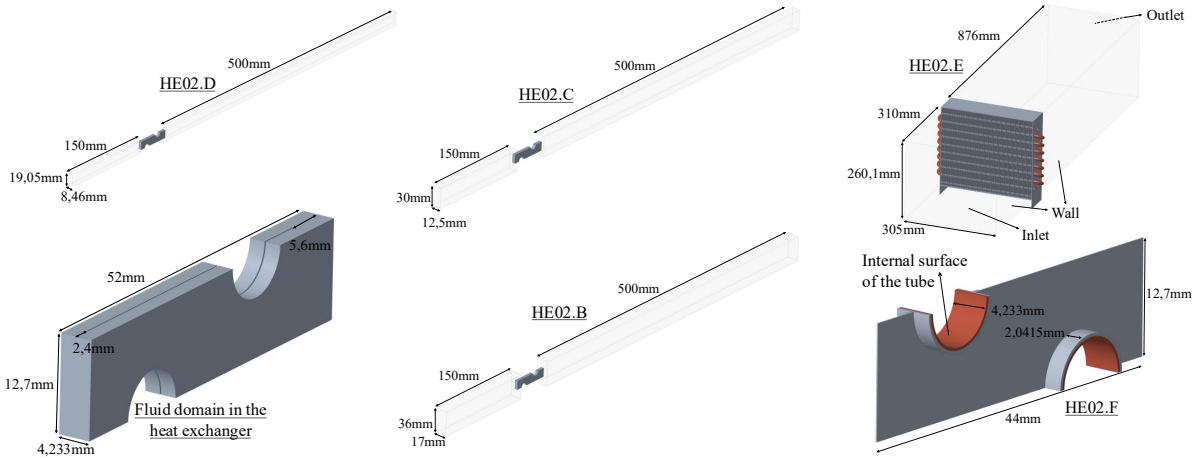

Figure 5. Models HE02.B, HE02.C, HE02.D (left) and versions HE02.E and HE02.F (right).

The analysis of the variable section simplified models' results allows to conclude that different inlet sections lead to distinct pressure drop behaviors due to the contraction and expansion effects of the flow when it gets to the exchanger/fin region. The HE02.D model (with smaller cross section area) is the one that approaches the most the full simulation version HE02.A (for aa 170 m³/h volumetric flow rate, the result of the HE02.D model was 12,1% higher than the HE02.A version, while for 510 m³/h the difference was 9,2%).

It can be verified through Figure 6 that when there is no alteration in the flow's cross section, the simplified version HE02.F can reproduce with high fidelity the experimental behavior. Besides, both computational models have certain capacity to reproduce the real behavior (in comparison to the constant section experimental test), especially for lower volumetric flow rates. Therefore, for a given constant section application throughout the domain, the simplified model HE02.F can reproduce the phenomenon with a maximum error of 10%. It is possible to conclude from the Fanning friction factor graphic from Figure 6 (right) that the simplified model HE02.F can reproduce with a good approximation the experimental data, even better than the constant section model (HE02.E). This difference in the results of the models

HE02.E and HE02.F may be associated to the fact that it is possible to obtain a better mesh refinement when working with the F model, due to its smaller size. The Fanning friction factor error for the E model, in relation to experimental data, is at most 25%.

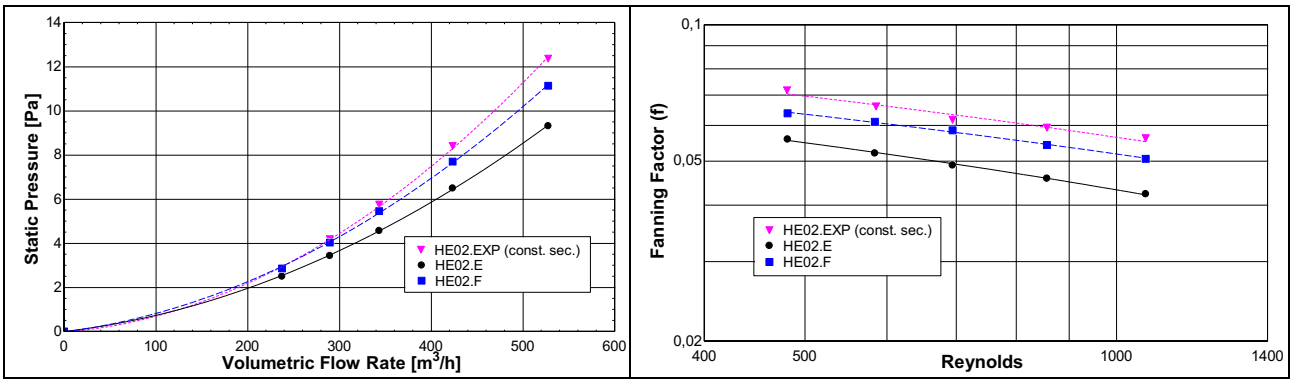

Figure 6. Pressure as a function of volumetric flow (left) and Fanning factor (f) as a function of Reynolds (right) for models HE02.E, HE02.F and experimental results.

To the thermal analysis, it was necessary to add the solid components (fins, tubes and plates of the heat exchanger) in the models. Hence, it was sought to evaluate two conditions: a prescribed temperature in the tube's internal surface (HE02.F) and a convection condition on the same surface (HE02.G), with a heat exchange coefficient h determined through the Gnielinski (1976) correlation. The results are shown in Table 2. For these models, three different flow rate conditions, 173, 340 and 510 m^3/h.

Table 2. HE02.F (left) and HE02.G (right) results.

Parameter	Unit	#1	#2	#3
Air side				
Flow rate	kg/s	1,14E-04	7,57E-05	3,86E-05
Flow rate	m^3/h	509,7	339,8	173,13
Velocity	m/s	1,78	1,19	0,61
Inlet temperature	°C	22,20	21,60	20,90
Outlet temperature	°C	29,35	30,03	32,37
Pressure Drop	Pa	8,86	4,50	1,51
Water side				
Surface temperature	°C	38,55	38,45	39,30
Results				
Heat transfer rate ($\dot{Q}_a$)	W	0,816	0,642	0,444
G	kg/sm²	3,66	2,44	1,24
Re	-	991,1	661,2	336,1
Effectiveness	-	0,438	0,500	0,623
NTU	-	0,576	0,694	0,976
UA	W/K	0,066	0,053	0,038
f	-	0,0446	0,0509	0,0658
j	-	0,0133	0,0160	0,0225

Parameter	Unit	#1	#2	#3
Air side				
Flow rate	kg/s	1,14E-04	7,57E-05	3,86E-05
Flow rate	m^3/h	509,7	339,8	173,13
Velocity	m/s	1,78	1,19	0,61
Inlet temperature	°C	22,20	21,60	20,90
Outlet temperature	°C	28,94	29,59	31,88
Pressure Drop	Pa	8,86	4,50	1,51
Water side				
h convection	W/m²K	6740,8	5602,2	4340,9
Surface temperature	°C	38,55	38,45	39,30
Results				
Heat transfer rate ($\dot{Q}_a$)	W	0,769	0,608	0,426
G	kg/sm²	3,66	2,44	1,24
Re	-	991,1	661,2	336,1
Effectiveness	-	0,412	0,474	0,597
NTU	-	0,531	0,642	0,908
UA	W/K	0,061	0,049	0,035
f	-	0,0446	0,0509	0,0658
j	-	0,0122	0,0148	0,0209

Analyzing the results depicted in Figure 7, it is possible to infer that the full model HE02.E is extremely similar to the experimental one, with an error inferior to 4%. Meanwhile, the simplified versions presented higher difference on the results when compared to the experimental data. It is important to notice that in the real version and in the full simulation model of the heat exchanger 02, four out of twenty tubes do not exchange heat, an effect that the simplified version can't reproduce. Consequently, the higher heat transfer presented in the simplified models is due to this fact (heat exchanger 03 does not possess this feature and its evaluation will allow to better quantify the performance of the simplified models).

When comparing the result of the simplified models, it is noticed that the boundary condition of prescribed temperature in the tube's internal surface is not adequate for this case, leading to errors of approximately 25%. Nevertheless, when the internal convection boundary condition is applied, the phenomenon is better represented, since it considers the internal thermal resistance of the tube, which affects the global performance of the heat exchanger. Overall, the HE02.G (convection) approach was deemed as most adequate for the simplified model's construction.

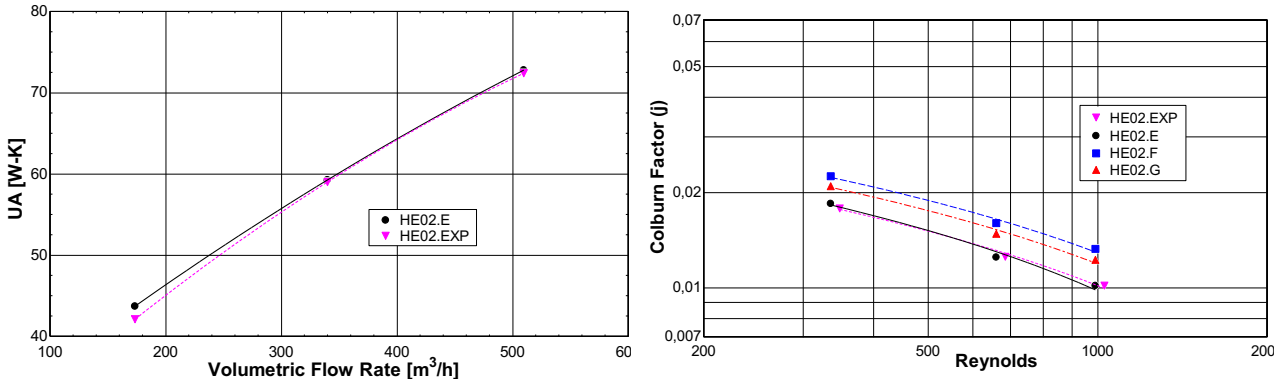

Figure 7. Global conductance as a function of volumetric flow (left) and Colburn factor (j) as a function of Reynolds (right).

3.3 Experimental/Numerical model HE03

The analysis performed in the heat exchanger 03 was thermal-focused. That being the case, the UA as a function of flow rate curve (Figure 8) was constructed and then the error of the full model with constant section (HE03.A) in relation to the experimental data for the flow rates of 170, 340 and 510 m³/h was quantified; the results were 4,7%, 3,9% and 2,5% respectively. Hence, the full model can reproduce the physical phenomenon with high accuracy. Figure 8 (right) shows the Colburn factor (j), from which the simplified model with prescribed temperature (HE03.B – equivalent in terms of construction and geometry to the HE02.F model) is further than the other results, as it tends to overestimate the real capacity of the heat exchanger's heat transfer rate, as previously discussed in the analysis of the heat exchanger 02. Overall, the results obtained in the simplified version with the convection boundary condition (HE03.C) were closer to the experimental data, so that the maximum error was 8,7%.

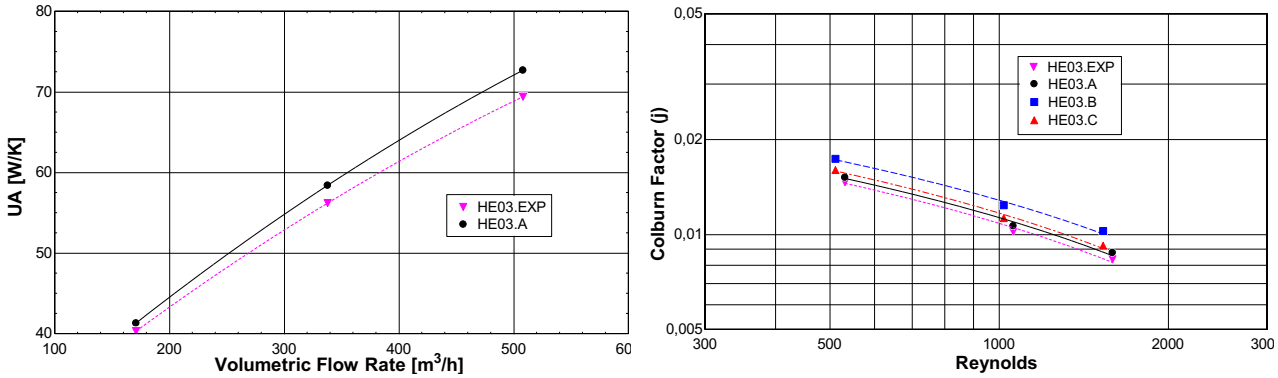

Figure 8. Global conductance as a function of flow rate (left) and Colburn factor (j) as a function of Reynolds (right).

4. CONCLUSIONS

Through several fluid dynamic simulations of the heat exchangers, it was noticed that the *Realizable K-Epsilon High y+* turbulence/wall model led to results that were closer to the experimental ones. In addition, it was possible to confirm that in models where the inlet section is bigger than the heat exchanger's one, the pressure drop is higher in comparison to constant section models. Besides that, this study allowed to conclude that full simulation models with an inlet section equal to the wind tunnel's dimension were capable of reproduce the effects measured in the physical version. For the simplified version, that aims to reproduce the effect of the tunnel's inlet section, there is high sensitivity in the results, according to the area of the inlet section. When there is no change in the section of the flow, the simplified version reproduces with a good accuracy the behavior of the full model.

Using the analysis of the full models, it was possible to conclude that these can reproduce with great accuracy the experimental data, with an error inferior to 5% for the UA values. When considering the simplified versions, the

prescribed temperature boundary condition led to a difference of up to 20% in the value of j, while the maximum error was 8,7% for the convection case.

Overall, it is possible to establish the final method for the thermohydraulic characterization of fin tube heat exchangers. The studied heat exchanger can be modelled in a simplified way, considering the fluid domain walls as symmetry planes, while for the fins, tubes and heat exchanger's structure the boundary effect shall be taken into account. The indicated turbulence model is *Realizable K-Epsilon*, the wall treatment is *High y+* and the most appropriate boundary condition is to consider a prescribed convection in the tube's internal surface. To convert of the results of the simplified model to the full physical version, equations for j and f are employed, from which the mass flow rate is obtained through the G ($G = \dot{m}/A_{min}$) parameter. It is also necessary to know the geometrical parameters of the studied physical heat exchanger, such as the heat transfer area A_s, the minimum crossing area A_{min} and the area of the internal face of the heat exchanger A_f.

5. ACKNOWLEDGEMENTS

This work was carried out under the auspices of the National Science and Technology Institutes (CNPq 404023/2019-3, FAPESC 2019TR0846).

6. REFERENCES

ASHRAE 33, 2000. "Method of Testing Forced Circulation Air Cooling and Air Heating Coils". *American Society of Heating, Refrigeration and Air Conditioning Engineers*, Atlanta-GA, USA.

ASHRAE 41.2, 1987. "Standard Methods for Laboratory Airflow Measurement". *American Society of Heating, Refrigeration and Air Conditioning Engineers,* Atlanta-GA, USA.

ASHRAE Standard 37, 1988. "Methods of testing for rating electrically driven unitary air-conditioning and heat pump equipment". *American Society of Heating, Refrigeration and Air Conditioning Engineers,* Atlanta-GA, USA.

ASHRAE Standard 51, 1999. "Laboratory methods of testing fans for aerodynamic performance rating". *American Society of Heating, Refrigeration and Air Conditioning Engineers,* Atlanta-GA, USA.

Barbosa, Jr., J. R., Hermes, C. J. L e Melo, C., 2010. "CFD Analysis of Tube-Fin 'No-frost' Evaporators". *Journal of the Brazilian Society of Mechanical Sciences and Engineering*, v.32, n.4, p.445-453.

Kays, W.M., London, A.L., 1998. "Compact Heat Exchangers". 3rd Ed., Krieger, Malabar, FL. 335 p.

7. RESPONSIBILITY NOTICE

The authors are the only responsible for the printed material included in this paper.